Journal of Imaging Science and Technology® 55(4): 040304-1–040304-7, 2011.


# Ink Jet Printing for Functional Ceramic Coatings

**M. Vilardell, X. Granados▲, S. Ricart▲, R. Cobas, M. Arjona, T. Puig, and X. Obradors**
*Institut de Ciència dels Materials de Barcelona (ICMAB-CSIC), Campus de la Universitat Autònoma de Barcelona, E-08193 Bellaterra, Barcelona, Spain*
*E-mail: ricart@icmab.es*

**S. C. Hopkins and B. A. Glowacki**
*Department of Materials Science and Metallurgy, University of Cambridge, Cambridge CB3 0FS, United Kingdom*

**J. Bennewitz, M. Falter and M. Bäcker**
*Zenergy Power GmbH, Rheinbach, Germany*

**Abstract.** *The interest in functional ceramic coatings based on low cost and flexible manufacturing has been heightened by the effectiveness shown by chemical solution deposition of metal-organic salts, usually based on the use of spin coating, dip coating, or slot die coating techniques prior to thermal treatment to achieve decomposition of the starting salts. The possibility of implementing effective drop on demand systems in the manufacturing process allows a more efficient way to apply the precursor solution homogeneously onto the substrate, thus, enabling control of thickness of the ceramic coating, by controlling the drop size and the pitch of the printing pattern, among other manufacturing advantages such as control of solvent evaporation. In the present work, the authors report on their experiments concerning ink jet coating of functional complex ceramics for $La_{0.7}Sr_{0.3}MnO_3$ and $YBa_2Cu_3O_{7-x}$ layers and patterns over single crystal and polycrystalline substrates using an electromagnetic system and a single nozzle piezoelectric dispenser. Characterization of rheological properties of the developed ink and of the resulting coating by optical microscopy, x-ray diffraction, scanning electron microscopy, and magnetic behavior are reported. © 2011 Society for Imaging Science and Technology.*
[DOI: 10.2352/J.ImagingSci.Technol.2011.55.4.040304]

## INTRODUCTION

Functional electroceramic coatings are in the industrial scope for obtaining operative devices with specific performances based on their singular properties. Conductive, semiconductive, piezoelectric, ferroelectric, pyroelectric, positive thermal coefficient resistivity transition, magnetoresistive, superconducting are examples of a large variety of metal oxides' functionalities. These functionalities have opened the area for manufacturing of devices that can be integrated with the standard electronics to produce cheaper and more effective designs exploiting the electrical functionalities that the world of ceramics can offer, from energy harvesting to supermarket ticketing, from sound transducers to capacitors or actuators.

Fabrication of controlled functional ceramic layers allows production at industrial scale of devices that exploit their singular properties, providing an opportunity to develop specific manufacturing techniques that can achieve high quality, flexibility, and low cost. Functional ceramic coatings are being produced by CVD, Sputtering, Pulsed laser deposition (PLD), and several other techniques that require high vacuum and extremely pure environment. From these expensive coatings, a device can be built by using appropriate photolithographic techniques to produce an adequate functional pattern to be integrated into the full device which can, in turn, be drawn over the same substrate. Chemical solution deposition (CSD) has been demonstrated to be an efficient and powerful methodology to obtain good functional ceramic coatings.[1] Metal-organic solutions, corresponding to the selected ceramic precursors, are commonly used for painting the surface of the substrate in order that, after pyrolysis and growth processes, an epitaxial or polycrystalline layer can be produced according to the properties of both the substrate and the ceramic coating.

The method for coating the substrate with the precursor solution should achieve uniform and consistent covering of the surface and support stress during thermal treatment without cracking, buckling, or any alteration of layer thickness. Therefore, prior to pyrolysis, it is essential to control the surface properties and fluid dynamics of precursor solution. In terms of applicability of ink jet printing deposition, we need to improve the standard solutions used for CSD for spin coating or dip coating in different aspects: solutions need to be easy to handle and modify; rheologically adjustable after addition of adequate additives to accomplish the jetting requirements for coating; and, finally, chemically compatible with the allowable printheads.

In the framework of the EFECTS EU collaborative project, we are investigating the possibility to obtain $La_{0.7}Sr_{0.3}MnO_3$ (LSMO) layers and deposit LSMO and

▲IS&T Member.

Received Dec. 9, 2010; accepted for publication Mar. 31, 2011; published online Jul. 28, 2011
1062-3701/2011/55(4)/040304/7/$20.00.

$YBa_2Cu_3O_{7-x}$ (YBCO) patterns onto different single crystals and polycrystalline substrates. The former complex ceramic is a ferromagnetic compound that allows achieving a magnetoresistive effect. Thus, it can be considered for magnetic field sensing and for transducer manufacturing.[2] The latter system corresponds to the YBCO high temperature superconducting (HTS) material of high interest for electronic, communication, and energy technology applications.[3,4]

Large superconducting devices need kilometers of superconducting wires to carry electrical current in the range of 3 $MA/cm^2$, however, due to the granular microstructure of these superconducting materials on a microscopic scale, it has been shown that the maximum current they can carry decreases exponentially with misorientation angle between adjacent grains.[5–7] So, for optimal performances, the crucial requirement is to prepare a template material that provides in-plane and out-of-plane biaxial crystallographic texture. Then, it is required that the orientation of the underlying template be transferred to the YBCO film and, thereby, that YBCO films grow in near single-crystal orientation (epitaxial growth). This represents one potential way of achieving one of the most challenging objectives in single-crystal coating.

In this field, it is very important to reduce the ac losses in superconducting devices and, thus, increase the efficiency in generation, transport and distribution of electrical energy. For this purpose, we are interested in making YBCO tracks with different geometries that could considerably reduce ac losses in high critical current density superconducting devices.[8,9]

## EXPERIMENTAL

In order to form functional layers, appropriate solutions of ceramic precursors have been prepared for coating. In this study, we report on two precursor systems to provide LSMO layers and one for YBCO patterning. The first LSMO precursor solution is based on lanthanum, strontium, and manganese propionates[10] and the second system is based on acetates of these same metals.[11,12] For YBCO patterning, the solution is based on yttrium, barium, and copper trifluoroacetates.[13]

Appropriate inks need to have specific rheological parameters to control the deposition process. Viscosity of each precursor solution was evaluated using a Rheometer Haake Rheostress 600 system with PP60Ti plate and a gap of 200 $\mu$m in low shear rate conditions; surface tension of inks was measured using the pendant drop method, and wetting angles were quantified by means of the sessile drop technique using a DSA100 system.[14,15]

### *LSMO Propionate Precursor Solution*

Propionates of La, Sr, and Mn, were obtained and dried in vacuum for 12 h at 90°C. Adequate amounts to obtain the metal stoichiometry, $La_{0.7}$, $Sr_{0.3}$ and $Mn_1$, were weighed in order to obtain 10 ml solutions of concentration 0.03 M in Mn, using propionic acid as a solvent.

**Table I.** Rheological and wetting properties of 0.03 M LSMO propionate based ink.

| | |
|---|---|
| Viscosity (mPa·s) | 1.0 |
| Surface tension (mN/m) | 22.0 |
| Contact angle over $LaAlO_3$ (°) | 7 |
| Density (g/ml) | 0.990 |

**Table II.** Rheological and wetting properties of 0.038 M LSMO acetate based ink.

| | |
|---|---|
| Viscosity (mPa·s) | 3.2 |
| Surface tension (mN/m) | 25.3 |
| Contact angle over $LaAlO_3$ (°) | $<7$ |
| Density (g/ml) | 0.917 |

Rheological and wetting properties of the solution are summarized in Table I.

Due to the low viscosity of the solution, ethyleneglycol was added at 30% (w/w), thus, increasing the viscosity up to 5.2 mPa·s. To correct the increase of the wetting angle produced by the higher surface tension of the solution, 0.06% (w/w) of Triton 114 was added to maintain wettability of the solutions. Solutions were stable for more than 1 month. Longer times have not been tested.

### *LSMO Acetate Precursor Solution*

A more environmental friendly system based on acetates was prepared by dissolving Sr and La acetate salts in water containing glycine, and Mn acetate in water containing ethylenediaminetetraacetic acid. A solution of ethanol/water (10/90%) and polyethyleneglycol (PEG MW 20,000) was added to obtain the desired concentration and to control the rheological and wetting properties. For 0.038 M concentration in Mn, the rheological and wetting properties are summarized in Table II. Solutions tend to oxidize in contact with air. Hermetically sealed solutions under Ar were tested for a month.

### *YBCO Precursor Solution*

In order to adapt solutions that have been developed for spin coating for printing onto single-crystal substrates, 0.5 M YBCO anhydrous solution based on yttrium, barium, and copper trifluoroacetates was prepared according to a described procedure.[13] Changes in solvent from methanol to ethanol and addition of PEG MW 8000 were introduced to control the rheology. The rheological and wetting properties of this solution are listed in Table III.

### *Printing*

Deposition was performed on a proprietary mechanical system capable of working in a controlled atmosphere. Two kinds of single nozzle jetting devices can operate to test the inks. The first jetting device consists of a pressurized chamber with a 100 $\mu$m diameter nozzle. The nozzle can be opened by using an electromagnetic valve for a time in the

**Table III.** Rheological and wetting properties of 0.5 M YBCO ethanol based ink.

| | |
|---|---|
| Viscosity (mPa·s) | 3.0 |
| Surface tension (mN/m) | 21.3 |
| Contact angle over $LaAlO_3$ (°) | 16 |
| Density (g/ml) | 0.909 |

range of 500–1000 $\mu$s, so delivering a portion of the fluid. This system allows delivering drops at a volume in the range of tens of nanoliters according to the pressure in the chamber and the time and amplitude of the opening valve.

The second system is mounted on the same mechanical rig and consists of a commercial pipette with piezoelectric excitation thus configuring a piezodispenser. The dispenser we used has a nozzle of 60 $\mu$m diameter and can deliver drops with volume in the range of 40 pl. The volume can be tuned by controlling the amplitude and the time of the electric pulse, which triggers the drop.

Direct measurements of the drop volume have been performed by measuring the volume of ink used to perform a number of fired drops under the same conditions. The number of drops achieved in this manner was around $4 \times 10^6$. Stability of drop shape and drop size has been tested by stroboscopic lighting, synchronized with the drop triggering and with a strobe delay in the range of 100 $\mu$s. The drop position was registered in the computer by a 1.3 megapixel commercial camera with a high quality M12 lens and a focal length of 22 mm. Any variation in the sharpness of the picture when synchronization is achieved was detected, thus indicating that synchronization and drop formation is accurately repetitive. The drop speed was estimated in the range of 2–3 m/s.

Deposition was performed on square shaped, $5 \times 5$ mm$^2$ and $10 \times 10$ mm$^2$ $LaAlO_3$ (LAO) single-crystal substrates and $10 \times 10$ mm$^2$ polycrystalline alumina. Thermal treatment for LSMO was performed in a tubular oven up to 900°C in air. From 100°C, temperature was increased up to 400°C with a heating ramp of 0.5°C/min, then increased by 1°C increments in a subsequent ramp up to 900°C. The samples were maintained at this temperature for 5 h and then freely cooled down to room temperature. In the case of YBCO, two thermal treatments were performed in a tubular oven: the first one consisted of pyrolysis for 30 min at 310°C and, then, the second one corresponded to a growth process at up to 810°C, followed by an isothermal step lasting 3 h at up to 600°C when the oxygenation process starts. The sample was then cooled from 600 to 450°C, the next step being a dwell for 3.5 h at this last temperature, and finally the sample was allowed to reach room temperature.[16]

## RESULTS AND DISCUSSION

### *Electromagnetic Valve*

LSMO full layers and patterned coatings were produced; all of them were shown to be electrically conductive with resistances in the range of 10–100 kΩ as expected for LSMO. According to the drop pitch, it is possible to obtain continuous layers with thicknesses, which depend on the substrate, the concentration of the solution, and the shot density of drops (number of drops per surface unit). Adequate overlapping of drops should be obtained by adjustment in according to drop volume, solution used to print and desired thickness. In our case, the diameter of the drops is nearly 300 $\mu$m, and good coverage can be achieved with a drop pitch of 100–150 $\mu$m. Shown in Figure 1 is an LSMO continuous coating on an LAO single-crystal substrate obtained by jetting propionate based ink. The thickness of the layer is in the range of 300 nm, and it shows low porosity or it shows high density. The estimated drop volume in this case is in the range of 5 nl.

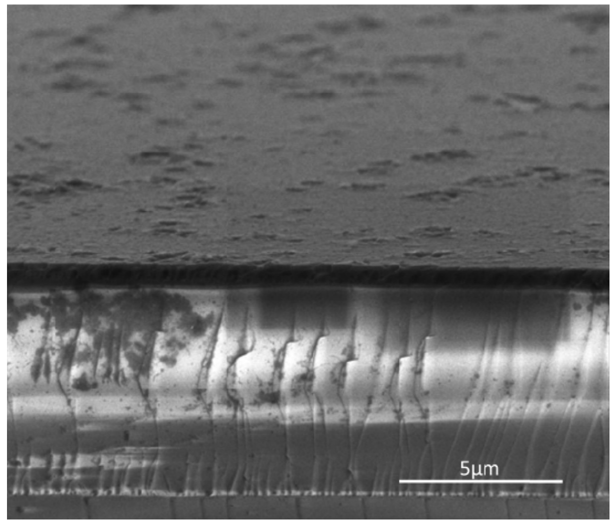


Figure 1. LSMO coating on LAO single-crystal substrate using LSMO propionate based ink.

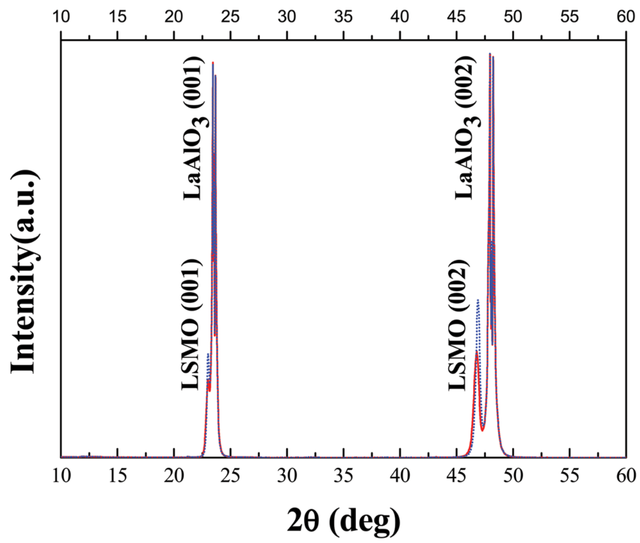


Figure 2. XRD diffraction patterns corresponding to a single (red solid line) and a double coating (blue dot line) using LSMO propionate based ink.

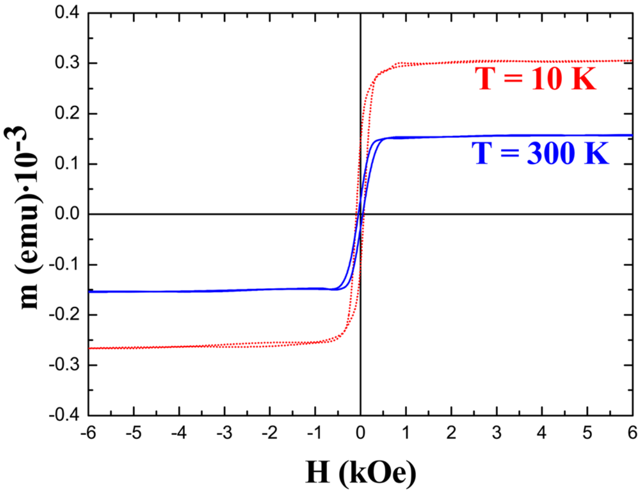


Figure 3. Magnetic moment of LSMO propionate based layer (see text). Magnetization curves have been measured at 300 K (blue solid line) and 10 K (red dot line) showing its ferromagnetic behavior.

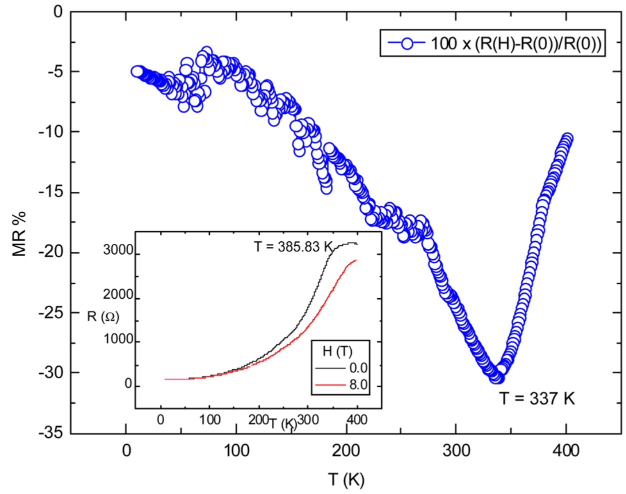


Figure 5. Magnetoresistive ratio of LSMO printed layers. At room temperature, the ratio achieves values nearly 30% for 8T magnetic field. Inset: resistance as a function of temperature for 0T (upper black curve) and 8T (lower red curve).

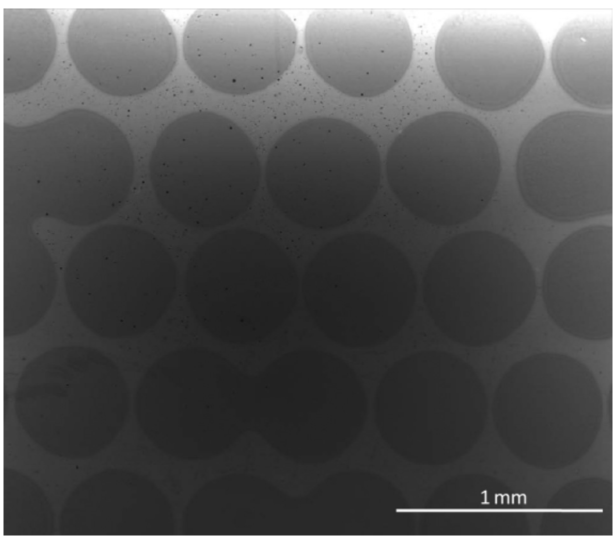


Figure 4. Scanning electron micrograph of LSMO dot patterned coating.

As can be seen in Figure 2, x-ray diffraction (XRD) pattern shows that LSMO layer has grown epitaxially, only (001) reflections can be observed, which we attribute to the low mismatch between LAO and LSMO cell parameters and growth dynamics, which allow crystal growth from the substrate interface. This epitaxial growth is realized from the precursor amorphous oxides obtained after pyrolysis of metal-organic salts present in the jetted ink. In this figure, the pattern is shown for a single layer coating (red solid line) and a double coating (blue dot line) obtained by first jetting an initial layer and second, after drying, an additional one on top. The layer obtained is also epitaxial as is shown in the XRD pattern in Fig. 2. The increase in amplitude of LSMO XRD peaks is in correspondence with increasing thickness.

The epitaxial layers so obtained show ferromagnetic behavior corresponding to the LSMO ceramic crystals. Shown in Figure 3 is the magnetic moment measured as a function of the applied magnetic field between −6 and 6 kOe at both temperatures 10 and 300 K. Saturation is observed at a field in the range of 0.5 kOe. The results are in agreement with those expected for this ceramic as reported elsewhere.[17]

Patterned layers have also been obtained by synchronizing the movement encoders with the triggering of the printhead driver. In this case, we used 0.038 M LSMO precursor acetate solution. In Figure 4, a pattern can be seen as made by independent drops with a pitch of 650 $\mu$m. The size of the drops is clearly visible, and it shows the high wettability of the substrate by the solution. The thickness in this case is in the range of 50 nm, six-fold thinner than the case depicted in Fig. 1 where the overlapping increases the amount of material for coating in a similar ratio. In order to obtain thicker drops than those in Fig. 4 it is necessary to increase the concentration of the solution or increase the surface tension of the solution to decrease spreading of the individual drops.

Epitaxial lines have also been obtained by ink jet printing with similar results.

Magnetoresistance was investigated in the LSMO epitaxial layers obtained by ink jetting of precursor ink followed by thermal treatment as specified above. In Figure 5, a typical evolution of the resistance is shown measured as a function of the temperature for two cases: with an external applied magnetic field of 8T (lower red curve), and without an external applied magnetic field (upper black curve).

### *Piezoelectric Dispenser*

The piezoelectric dispenser was also used to jet LSMO and YBCO inks over LAO substrates with similar results, but with a better capacity to disperse the ink on the substrate and trim the thickness by controlling the drop pitch. Optimum pitch for good overlapping was experimentally

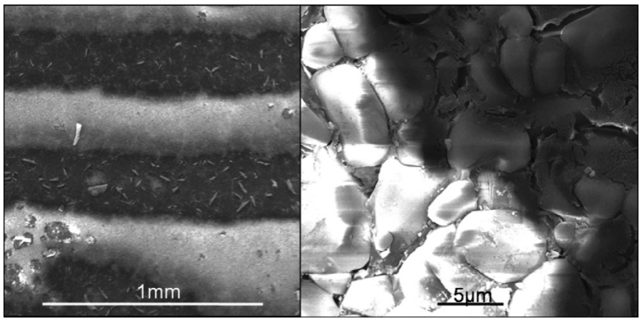


Figure 6. Detail of LSMO printed tracks over commercial alumina. Porosity of alumina causes stress in the thicker regions of the coating producing a peeling effect that can be observed on the left side. On the right, can be distinguished the behavior of the thin wetted parts, clearly opposite to that of the thicker ones where the stress produces dewetting.

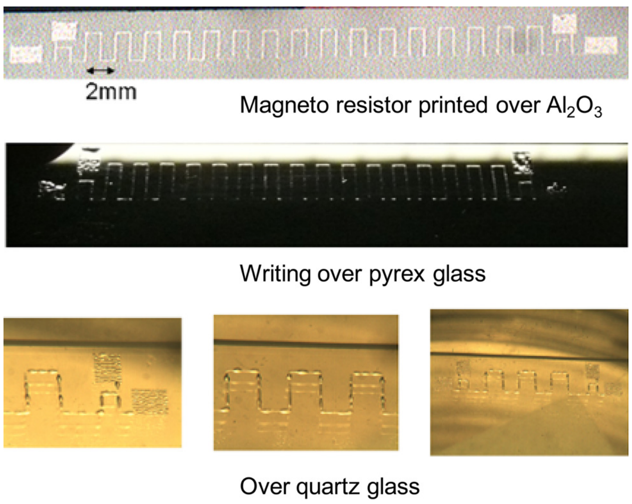


Figure 7. LSMO magnetoresistive devices printed over several substrates before thermal treatment. Beats are clear in the quartz glass substrate thus indicating that surface tension should be diminished or viscosity increased.

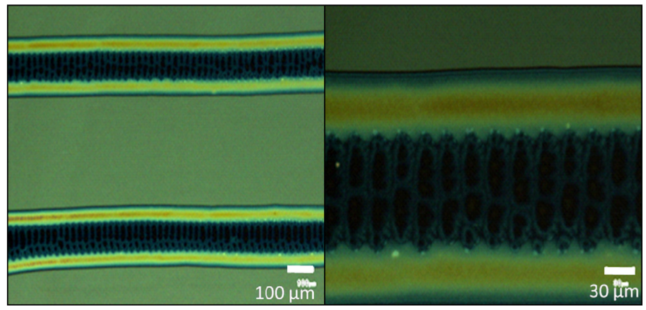


Figure 8. Optical micrographs of ink jet printed YBCO tracks on LAO substrate after pyrolysis, at 5× magnification (left) and 20× (right).

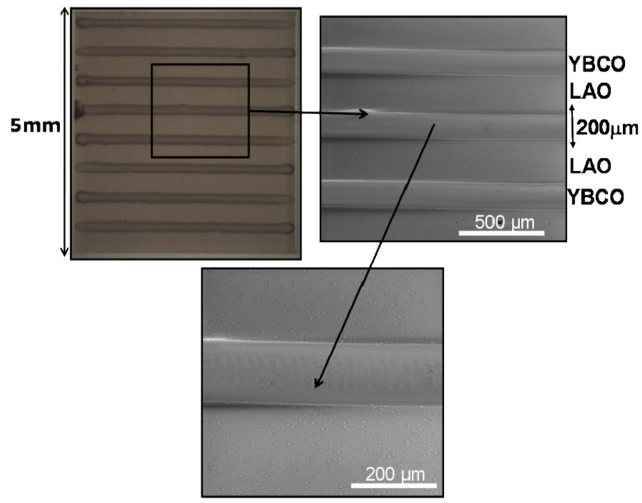


Figure 9. SEM images of ink jet printed YBCO tracks on LAO substrate after growth process.

established as 25 $\mu$m for 35–40 pl drops. Taking into account the evaporation rate of the solvent, the distribution of the ink along large areas can be controlled by pinning the liquid front with drops previously placed and partially dried. Due to the lower filling speed that can be achieved in this case and the lower volume of the drops, the evaporation rate of solvent is of great importance.

Due to electrical and magnetic properties of the LSMO system that are also observable in polycrystalline aggregates, an effort was made to determine its behavior on lower cost polycrystalline substrates. We have used standard alumina substrates of common application in electronics, and tracks have been printed on it using LSMO 0.1 M ink with rheological correction. Wettability of the alumina substrate was sufficient to allow a good layer of ink to be obtained. After heat treatment at 900°C in air, the tracks were electrically tested; electrical resistivity along them in the range of kilohm was observed.

The structure of the LSMO was observed by scanning electron microscopy (SEM) for tracks smaller than 250 $\mu$m in width. The layer thus obtained shows problems of delamination in parts where the thickness is higher, but the thinner parts of the track show good adherence. Figure 6 (left) shows the tracks with the "peeling" effect. A more detailed insight can be observed in Fig. 6 (right). The limit of the track can be seen over the grains of $Al_2O_3$, some of them being only half coated. Only over the pores, is the coating thick enough to connect the LSMO grains in a sponge-like structure. However, conductance testing shows that tracks are fully connected.

Printing of magnetoresistive devices based on square wave shaped lines with a period of 2 mm was also tested using different polycrystalline and amorphous substrates. In Figure 7, a set of three prints over alumina, Pyrex glass, and quartz glass is shown before thermal treatment. In this case, drop volume and surface tension have been modified to minimize spreading in order to achieve thin tracks. The hydrophilic character of alumina and Pyrex glass allows good adherence of the drops, meanwhile, the higher surface tension, in the range of 50 mN/m, tends to decrease the spreading of the drops. The width of the tracks obtained is around 100 $\mu$m. In the case of less hydrophilic quartz glass, the width of the tracks is smaller, which suggests that the

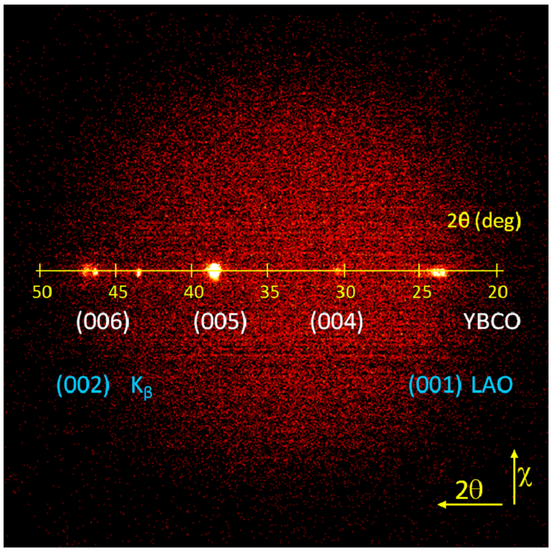


Figure 10. X-ray diffraction pattern of ink jet printed YBCO tracks on LAO substrate after growth process.

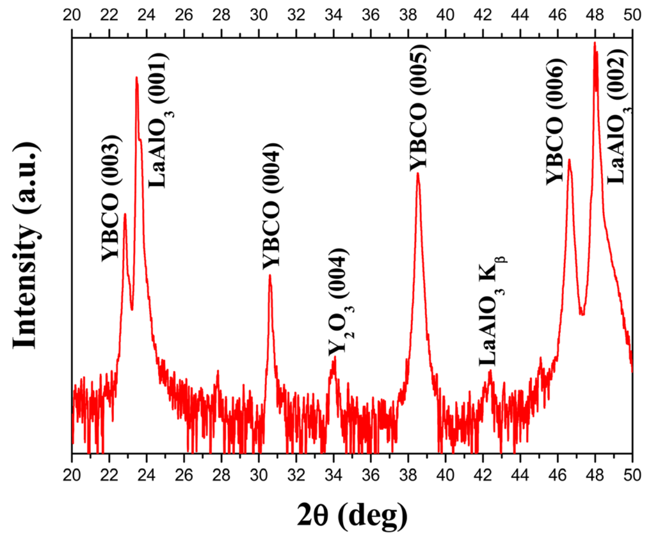


Figure 12. X-ray diffraction pattern corresponding to the institutional logo.

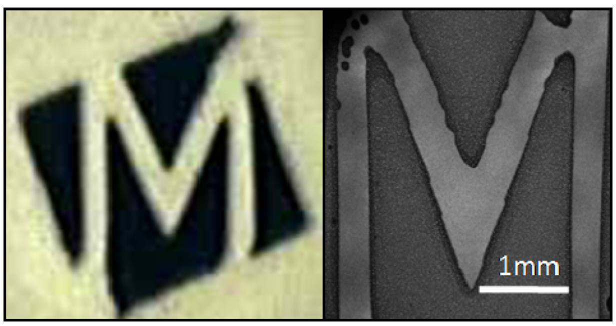


Figure 11. General aspect of YBCO institutional logo over LAO substrate by optical microscopy (left) and by scanning electron microscopy (right).

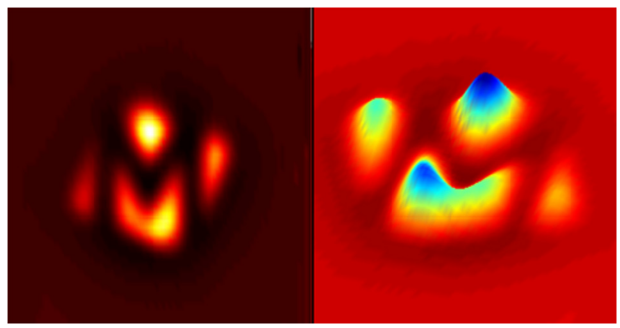

Figure 13. Hall magnetometry of trapped magnetic field in the patterned institutional logo after a field cooling process down to 77 K, below the superconducting transition temperature. It shows the typical field distribution as expected in a Bean context (see text).

width can be regulated by controlling the surface tension thereby minimizing the spread of ink. Beats can be observed, however, on the less hydrophilic quartz glass substrate; these could be corrected by diminishing the drop volume or increasing the viscosity of the solutions. Work is being done in order to address the problem. It is worth mentioning that transverse lines to the device have been drawn in rastering mode and the jetting applies drops in both directions. No misalignment is observed indicating that a high precision in synchronization should be achieved for the manufacturing of electronic devices based on functional ceramics. In our case, synchronization is based on pulses generated each 250 nm of displacement. The design includes the pads for electrical contacts.

In order to advance in HTS device manufacturing with low ac losses, YBCO straight lines and patterns were drawn on LAO substrate with a piezoelectric dispenser. Viscosity of ink was increased up to 3 mPa·s by addition of polyethyleneglycol. Printing feature was observed by optical microscopy after drying and a pyrolysis process at 310°C for 30 min (Figure 8). The lines obtained by overlapping of drops delivered each 25 $\mu$m show sharp edges and a homogeneous width of 200 $\mu$m. It is clear that contraction during drying and pyrolysis processes and a strong pinning of the edges induce a transversal stress, which we infer on the basis of the formation of a thin net of wire-like polymeric residuals, as can be seen in the optical micrographs shown in Fig. 8. YBCO growth, however, is epitaxial after an annealing treatment at high temperature (Figure 10). After this growth process, which is shown in the scanning electron micrographs in Figure 9, these wire-like transversal structures tend to vanish, achieving good homogeneity of the tracks. Lines with a width around 200 $\mu$m and a thickness value on the edge of the track around 80 nm were thereby obtained.

Two-dimensional XRD experiments (Fig. 10) have been performed in order to identify the composition and structure of the tracks. The XRD pattern shows the presence of (001) YBCO reflections, which means that YBCO has grown maintaining the same structure as the single-crystal LAO substrate, as expected from the low layer-substrate mismatch. Epitaxial growth occurs along the tracks regardless of the transverse stress on the tracks.

Apart from parallel lines, YBCO patterns have also been printed using the piezoelectric printhead. Figure 11 shows the results for the logo of our institution ink jet directly printed onto a $10 \times 10$ mm$^2$ LAO substrate.

This previous pattern was grown using the same thermal treatment mentioned before for the YBCO tracks, and then it was characterized by XRD, showing, as happened for the previous tracks, a YBCO epitaxial growth, (001) YBCO[100]||(001)LAO[100], as depicted in Figure 12.

Also, magnetic measurements have been performed by Hall magnetometry showing YBCO is homogeneous in the connected parts of the superconducting pattern (Figure 13).The distribution of trapped magnetic field once the superconducting state was achieved in a field cooling process to 77 K is in good agreement with that expected from the Bean approach.[18–20] As can be observed in the left-most map, the field distribution shows homogeneity in the superconducting islands. The right figure shows the intensity of the trapped magnetic field on a three-dimensional basis.

## CONCLUSIONS

The present work shows the feasibility of using CSD precursors by adapting their rheology and selecting the appropriate solvent and additives for ink jet printing. The control of ink rheology and wetting parameters has been shown to be crucial for the full and patterned coatings. In the case of LSMO ceramic oxide, two types of metal-organic precursors have been adapted for jetting in different printheads. Epitaxial LSMO growth has been achieved in both full and patterned coating leading to the possibility of building up on board electronic components in a full ink jet manufacturing philosophy. The set of precursor inks can be extended for jetting over polycrystalline substrates, but caution should be taken with the high roughness of these substrates in order to avoid stress-induced dewetting. Functional superconducting epitaxial coating has also been demonstrated using appropriate precursor inks for printing both tracks and extended patterns.

It is worth mentioning that ink jet technology provides an easy and cheaper way for building electronic and magnetic devices integrating functional ceramics. Integration of functional components in a full printed electronic system is stressed by combining patterned sensing devices based on specific functional materials with complementary electronics that nowadays are being developed for ink jet printing manufacturing, in the same way as for low cost radio frequency identification systems.

## ACKNOWLEDGMENTS

The authors would like to acknowledge the financial support from Spanish MICCIN (CONSOLIDER NANOSELECT CSD2007-0041), Generalitat de Catalunya (Pla de Recerca SGR-0770 and XaRMAE), and EU (EFECTS FP7-NMP-2007-SMALL-1, NESPA).

## REFERENCES

[1] X. Obradors, T. Puig, A. Pomar, F. Sandiumenge, N. Mestres, M. Coll, A. Cavallaro, N. Roma, J. Gazquez, J. C. Gonzalez, O. Castano, J. Gutierrez, A. Palau, K. Zalamova, S. Morlens, A. Hassini, M. Gibert, S. Ricart, J. M. Moreto, S. Piñol, D. Isfort, and J. Bock, "Progress towards all-chemical superconducting YBCO coated-conductors", Supercond. Sci. Technol. **19**, s13 (2006).

[2] A. M. Haghiri-Gosnet and J. P. Renard, "CMR manganites: Physics, thin films and devices", J. Phys. D: Appl. Phys. **36**, 127–150 (2003).

[3] D. C. Larbalestier, A. Gurevich, D. M. Feldmann, and A. Polyanskii, "High-$T_c$ superconducting materials for electric power applications", Nature (London) **414**, 368 (2001).

[4] M. Paranthaman and T. Izumi, "High-performance YBCO-coated superconductor wires", Mater. Res. Bull. **8**, 533 (2004).

[5] D. Dimos, P. Chaudhari, J. Mannhart, and F. K. Legoues, "Orientation dependence of grain-boundary critical currents in $YBa_2Cu_3O_{7-\delta}$ bicrystals", Phys. Rev. Lett. **61**, 219 (1988).

[6] A. Goyal, M. Paranthaman, and U. Schoop, "The RABITS approach: Using rolling-assisted biaxially textured substrates for high-performance YBCO superconductors", Mater. Res. Bull. **8**, 552 (2004).

[7] Y. Iijima, K. Kakimoto, Y. Yamada, T. Izumi, T. Saitoh, and Y. Shiohara, "Research and development of biaxially textured IBAD-GZO templates for coated conductors", Mater. Res. Bull. **8**, 564 (2004).

[8] O. Tsukamoto and M. Ciszek, "AC magnetization losses in striated YBCO-123/Hastelloy coated conductors", Supercond. Sci. Technol. **20**, 974–979 (2007).

[9] W. T. Norris, "Calculation of hysteresis losses in hard superconductors carrying AC: Isolated conductors and edges of thin sheets", J. Phys. D. **3**, 489–507 (1970).

[10] U. Hasenkox, C. Mitze, and R. Waser, "Metal propionate synthesis of magnetoresistive $La_{1-x}(Ca,Sr)_xMnO_3$", J. Am. Ceram. Soc. **80**, 2709–2713 (1997).

[11] S. M. Liu, X. B. Zhu, J. Yang, B. C. Zhao, Z. G. Sheng, W. H. Song, J. M. Dai, and Y. P. Sun, "Fabrication of polycrystalline $La_{0.7}Sr_{0.3}MnO_3$ thin films on Si (100) substrates by chemical solution deposition", Physica B **353**, 238–241 (2004).

[12] Z. J. Wang, H. Usuki, T. Kumagai, and H. Kokawa, "Microstructure and electrical properties of lead zirconate titanate thin films deposited by sol-gel method on $La_{0.7}Sr_{0.3}MnO_3/SiO_2/Si$ substrate", J. Sol-Gel Sci.Technol. **42**, 375–379 (2007).

[13] N. Roma, S. Morlens, S. Ricart, K. Zalamova, J. M. Moreto, A. Pomar, T. Puig, and X. Obradors, "Acid anhydrides: A simple route to highly pure organometallic solutions for superconducting films", Supercond. Sci. Technol. **19**, 521 (2006).

[14] A. W. Adamson, *Physical Chemistry of Surfaces*, 5th ed. (Wiley, New York, 1990).

[15] D. Myers, *Surfaces, Interfaces and Colloids. Principles and Applications*, 2nd ed. (Wiley-VCH, New York, 1999), pp.140–161.

[16] A. Llordes, K. Zalamova, S. Ricart, A. Palau, A. Pomar, T. Puig, A. Hardy, M. K. Van Bael, and X. Obradors, "Evolution of metal-trifluoroacetate precursors in the thermal decomposition towards high performance $YBa_2Cu_3O_7$ superconducting films", Chem. Mater. **22**, 1686–1694 (2010).

[17] K. Dörr, "Ferromagnetic manganites: Spin-polarized conduction versus competing interactions", J. Phys. D: Appl. Phys. **39**, 125–150 (2006).

[18] C. P. Bean, "Magnetization of hard superconductors", Phys. Rev. Lett. **8**, 250 (1962).

[19] M. Carrera, X. Granados, J. Amorós, R. Maynou, T. Puig, and X. Obradors, "Computation of critical current in artificially structured bulk samples from Hall measurements", IOP J. Phys. Conf. Ser. **97**, 012107 (2008).

[20] M. Carrera, X. Granados, J. Amorós, R. Maynou, T. Puig, and X. Obradors, "Detection of current distribution in bulk samples with artificial defects from inversion of Hall magnetic maps", IEEE Trans. Appl. Supercond. **19**, 3553 (2009).